Supporting information available:

- Notes on the real and imaginary parts of the complex viscosity
- Frequency dependence of the magnetoviscous effect
- Reversibility of magnetoviscosity upon on/off switching of the applied magnetic field
- Genetically engineered TMV variants with altered surface chemistries and charges
- Visualization of TMV/ferrofluid microstructures using optical microscopy

Notes on the real and imaginary parts of the complex viscosity

During measurement in the PMAV, our samples are confined between two horizontal plates in a narrow gap, with the lower plate induced to impose a small-amplitude sinusoidal strain in the vertical direction by a piezoelectric actuator driven at frequencies between 8 and 200 Hz. The corresponding stress is detected by piezoelectric sensors and converted into the complex modulus G^*. The quantity G^* is often written in the form $G^*(\omega) = G'(\omega) + iG''(\omega)$, where *i* is the imaginary unit and ω denotes angular frequency (2π times the oscillation frequency f). The first term on the right-hand side, $G'(\omega)$, is called the *storage modulus*, while the second term, $G''(\omega)$, is referred to as the *loss modulus*. The storage modulus is a measure for the storage of elastic energy in the sample, whereas the loss modulus is proportional to the viscous dissipation of energy.

The complex viscosity is defined by

$$\eta^* = \eta' - i\eta'' = \frac{G^*(\omega)}{i\omega} = \frac{G''(\omega)}{\omega} - i\frac{G'(\omega)}{\omega}.$$

Therefore, $\eta' = \frac{G''}{\omega}$ and $\eta'' = \frac{G'}{\omega}$.

Frequency dependence of the magnetoviscous effect

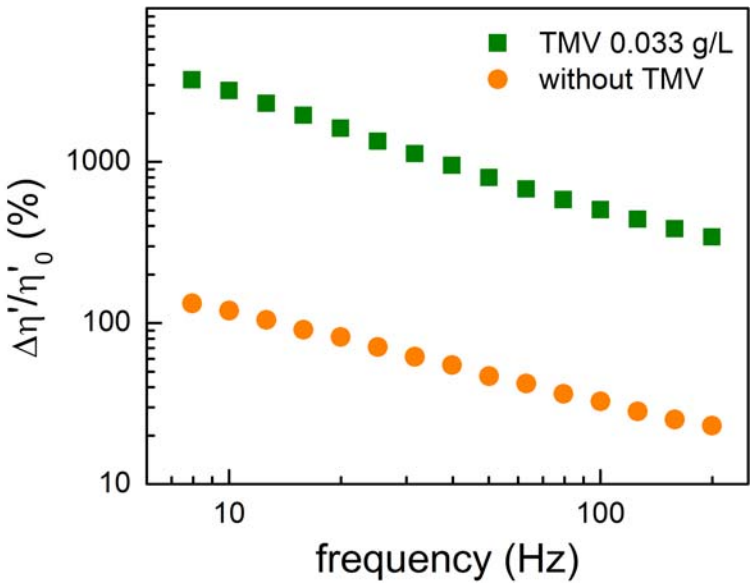

Figure S1. The magnetoviscous effect plotted against vibrational frequency for ferrofluids with and without TMV additive at an applied magnetic field of 110 mT. The ferrofluid containing TMV (green squares) manifests an enhanced magnetoviscous effect throughout the measured frequency range, with the magnetoviscosity exceeding 300% at f = 200 Hz, compared to only 20% in the sample without TMV. This indicates that the increased magnetoviscosity imparted by the presence of TMV is retained even at high shear rates.

Reversibility of magnetoviscosity upon on/off switching of the applied magnetic field

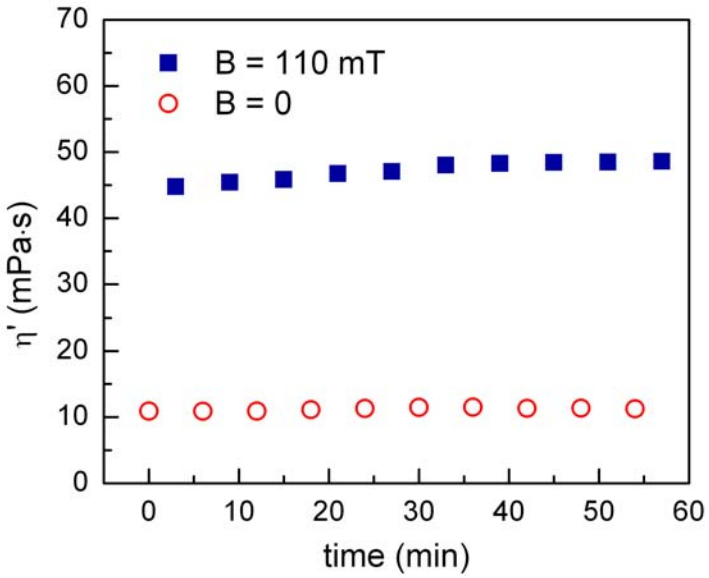

Figure S2. Magnetoviscosity measured after switching a magnetic field of 110 mT on and off 10 times within 57 minutes. The viscosity took on constant values in both the field-on and field-off states, regardless of prior history. All measurements were carried out at a vibrational frequency of 10 Hz.

Genetically engineered TMV variants with altered surface chemistries and charges

Production and purification of surface mutants of *Tobacco mosaic virus* (TMV_{Lys} and TMV_{Cys}) have been described in detail by Geiger (2010). Tabakmosaikvirus-Hüllproteinvarianten als Bausteine für die Nano- und Arraytechnologie (*Tobacco mosaic virus coat protein variants - a toolbox for nano- and array technology applications*), PhD thesis; Arbeiten und Mitteilungen aus dem Biologischen Institut der Universität Stuttgart 45 ISSN 0723-2055. This work will be published in English elsewhere.

Whereas natural TMV was isolated from tobacco plants at 21 days post inoculation using the method of Devash et al. (1981) with minor modifications, purification of genetically engineered particles of TMV surface mutants produced in plants followed the protocol of Gooding and Hebert (1967), which was also applied to natural (wild-type) TMV for experiments carried out in parallel with both natural and modified TMV variants.

References for TMV purification protocols:

Y. Devash, A. Hauschner, I. Sela, K. Chakraburtty (1981). The Antiviral Factor (AVF) from Virus-Infected Plants Induces Discharge of Histidinyl-TMV-RNA; *Virology* **111**, 103-112.

G. V. Gooding, T. T. Hebert (1967). A simple technique for purification of tobacco mosaic virus in large quantities; *Phytopathology* **57**, 1285.

Visualization of TMV/ferrofluid microstructures using optical microscopy

As illustrated in Figure S3, optical microscopy of LCE-25 ferrofluid samples both with and without TMV reveals that the addition of virus nanotubes increases the size of agglomerates that form upon the application of a magnetic field; in the absence of a magnetic field, the agglomerates observed in both samples were similar in size. Sosnick *et al.* (Ref. 44 in the manuscript) studied magnetic field-induced microstructures of TMV/ferrofluid composite materials using small-angle neutron scattering. The orientation distribution of scattering intensities from such samples yielded direct evidence for the alignment of TMV particles parallel to the applied magnetic field. In the absence of magnetic particles, no apparent field-induced alignment of TMV was observed. Presumably, the interaction of the magnetic particles with TMV is responsible for both the alignment of the virus nanotubes and the agglomerate structures that are visible in the optical micrographs.

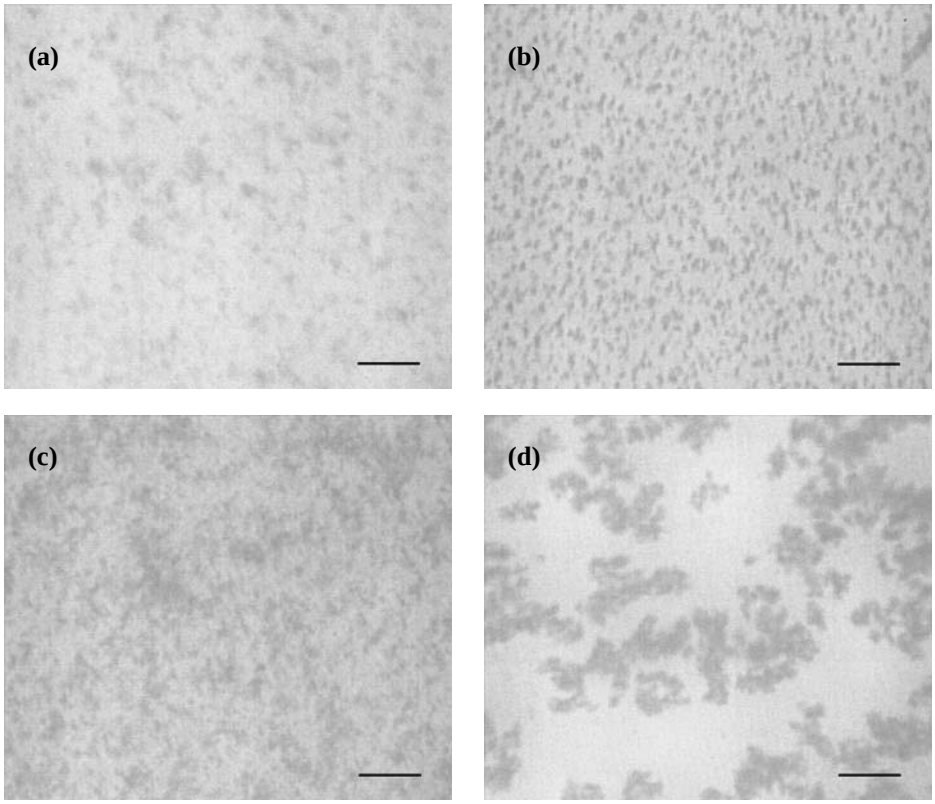

Figure S3. Visualization of microstructures in ferrofluid samples by reflected-light optical microscopy, in the absence or presence of a magnetic field oriented perpendicularly to the sample slide. (a) LCE-25 without TMV, no magnetic field; (b) LCE-25 without TMV, magnetic field applied; (c) LCE-25 with TMV, no magnetic field; (d) LCE-25 with TMV, magnetic field applied. At zero field ((a) and (c)), no significant difference in the average size of particle agglomerates was detected. In a magnetic field ((b) and (d)), TMV additives caused extensive agglomeration of $CoFe_2O_4$ particles. The magnitude of the applied magnetic field applied was not quantified (FeNd permanent magnet, positioned directly under the ferrofluid sample). Scale bars: 100 μm.